Reliability Evaluation of Grid-Connected Photovoltaic Power Systems

Peng Zhang, *Senior Member, IEEE*, Yang Wang, Weidong Xiao, *Member, IEEE*, and Wenyuan Li, *Fellow, IEEE*

***Abstract*—This study presents a systematic way to evaluate reliability performance of large grid-connected photovoltaic (PV) power systems considering variation of input power and ambient-condition-dependent failure rates of critical components including PV modules, inverters, and capacitors. State enumeration is used to analyze real-life grid-connected PV systems. Ambient-condition-dependent failure rates of major components in PV systems are formulated and incorporated in reliability analysis. A series of reliability indices are defined to quantify PV systems' reliability performance. In addition, sensitivity analyses are extensively conducted to investigate the impact of different factors on the performances of PV power systems. Test results on a practical 20-kW PV project are presented to demonstrate the effectiveness of the proposed method.**

***Index Terms*—Inverter, photovoltaic (PV) system, reliability, sensitivity, state enumeration.**

I. Introduction

ELECTRICITY generated from photovoltaic (PV) power systems is a major renewable energy source which involves zero greenhouse gas emissions and no fossil fuel consumptions. The total capacity of grid-connected PV power systems have grown exponentially from 300 MW in 2000 to about 21 GW in 2010 [1]. A 60% average annual growth rate of PV capacity has been seen from 2004 through 2009, and an 80%–90% growth is anticipated in 2011. Highly reliable PV power systems, therefore, will greatly increase renewable energy output, guarantee higher return on investment, and help curtail carbon emissions globally.

Similar to any other electrical systems, grid-connected PV power systems can fail because of accidental events and occasional failures in its components, resulting in significant amounts of economic loss [2]. Hence the reliability of grid-connected PV power systems has been of great concern to both utility companies and customers [3]. Normally, a PV power system is composed of many vulnerable components [4], such as power electronic devices and solar cells [5], whose lifecycle reliability is highly dependent on loads and ambient conditions. The complex nature of PV power systems makes it challenging to quantify the reliability of the entire generation station. The existing literature mostly focuses on reliability assessment for power electronic components such as IGBT [6], capacitor [7], and inverter [8], whereas much fewer references discuss the reliability evaluation for the entire PV system. References [9] and [10] presented simplified, system-level models for PV system reliability using the Markov concept. Hierarchical reliability block diagram was developed in [11] to model the behavior of the PV system. Important contributions to PV reliability modeling have been presented in [2] and [12], where the impact of inverter failures on total lifetime of the PV system is quantified by using Monte Carlo simulation. In the above literature, failure rates or probabilities of electronic elements in the PV system are treated as constants. These reliability parameters, however, are actually varying with system states including solar insolation, ambient temperature [13], and load level [14], etc.

This paper proposes a systematic reliability evaluation method for large-scale commercial and utility-level PV power systems. A major contribution of this paper is the quantification of the impact of input power levels on the failure rates of critical components such as PV modules, inverters, and capacitors. Existing grid-connected systems are normally connected in a centralized structure or its variants, which use a single middle or large-sized inverter dedicated to a series of PV panels. The proposed method is described using the central inverter topology. A state enumeration technique is developed to analyze real-life central inverter topology. It is easy to apply the method to other topologies [15] since the state enumeration is flexible to handle any structure. Ambient-condition-dependent failure rates of major components in the PV system are formulated. A set of metrics are presented to quantify PV system reliability and impacts of reliability on PV system operation and energy output. In addition, sensitivity analyses are extensively conducted to explore the effects of different factors on the performances of PV power systems, which serves a useful guide for PV system design, operation, and maintenance.

The organization of this paper is as follows. Reliability modeling of PV system components is introduced in Section II. Section III describes a method to build discrete probability distribution of input power. PV reliability indices are presented in Section IV. Test results are summarized in Section V, followed by conclusions in Section VI.

II. Reliability Modeling of PV System Components

The overall picture of a large grid-connected PV system is investigated first, before going into details of PV reliability assessment. As shown in Fig. 1, the three-phase central inverter PV system consists of three PV arrays. For each array, n PV

Manuscript received August 25, 2011; revised December 06, 2011; accepted January 28, 2012. Date of publication April 13, 2012; date of current version June 15, 2012.

P. Zhang and Y. Wang are with the Department of Electrical and Computer Engineering, University of Connecticut, Storrs, CT 06269 USA (e-mail: peng@engr.uconn.edu; yaw11002@engr.uconn.edu).

W. Xiao is with the Program of Electrical Power Engineering, Masdar Institute of Science and Technology, Abu Dhabi, UAE (e-mail: mwxiao@masdar.ac.ae).

W. Li is with BC Hydro and Power Authority, Vancouver, BC, V7X 1V5, Canada (e-mail: wen.yuan.li@bchydro.com).

Color versions of one or more of the figures in this paper are available online at http://ieeexplore.ieee.org.

Digital Object Identifier 10.1109/TSTE.2012.2186644

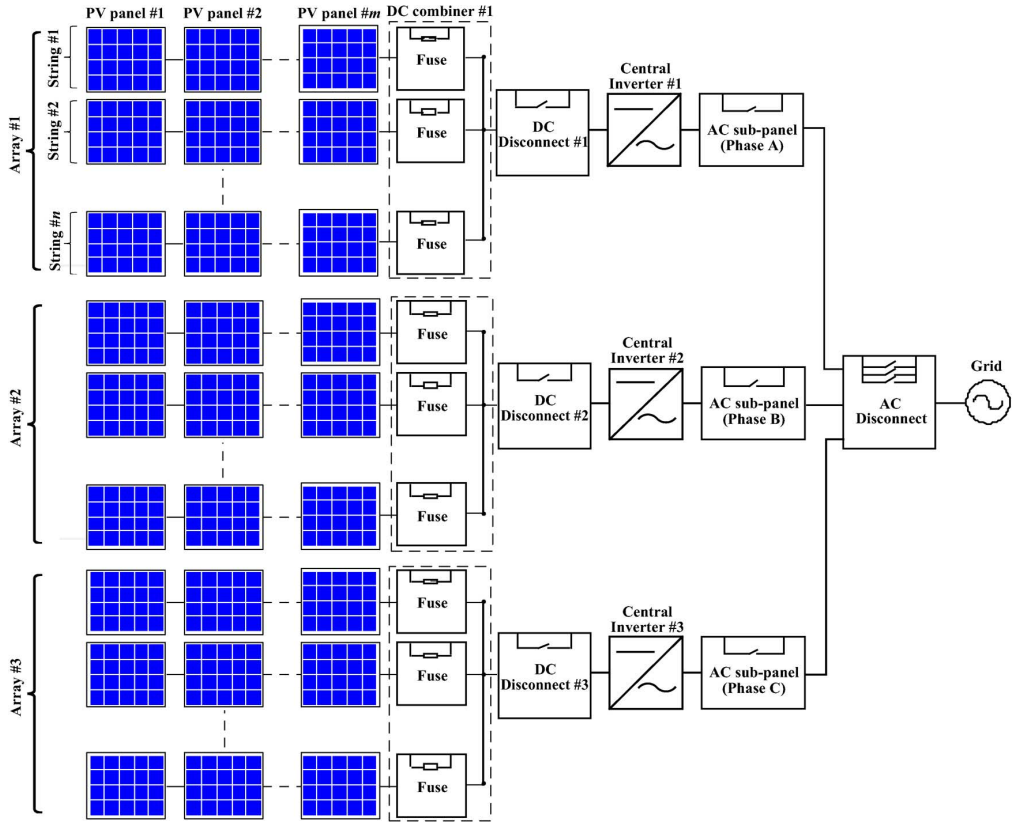

Fig. 1. Schematic diagram of a PV power system using central inverters.

strings are connected to a dc combiner including a fuse and other protection devices. DC energy generated from PV arrays flows through dc disconnects, which creates visible gaps under contingencies to isolate PV arrays from the system. The central inverter delivers ac power for the entire phase, normally at 208 V, through an ac subpanel to an ac disconnect or breaker, which eventually sends three-phase power to the utility system.

A two-step approach is adopted for the reliability evaluation of the large-scale commercial PV systems. First, a reliability model of each component in Fig. 1 is analyzed and parameterized. Then, the system-level reliability is computed using network reliability theory [16], as discussed in Sections III and IV.

A. Reliability Evaluation of PV Inverter

Inverters are among the vulnerable components in PV power systems. A PV inverter may handle a high level of power flow and operate under high temperature environment, incurring higher energy losses in semiconductor switches and capacitors. High energy losses inevitably increase the core temperature of switching devices, which degrades the inverter reliability and increases the risk of component aging failures. Obviously, the reliability of the PV inverter is highly dependent on solar light intensity, ambient temperature, and input power levels. An analysis approach is proposed to quantify the power input related failure rates of inverter components as follows.

1) Thermal Model of IGBT and Diode: A typical single-phase inverter consists of a connection of IGBTs and diodes, as shown in Fig. 2. A series of empirical formula have been

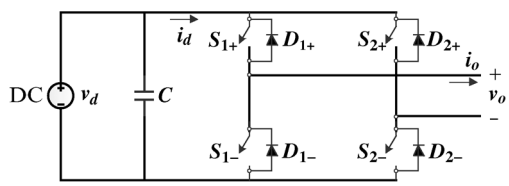

Fig. 2. Single-phase full-bridge inverter topology.

proposed for estimating power losses in IGBTs and diodes [17], which are briefly summarized in the Appendix.

Given the power losses, the temperature rise in IGBT and diode can be calculated by the following linear heat transfer equations [17], [18]:

$$\Delta T_{\mathrm{IGBT}} = \theta_{11} P_{\mathrm{IGBT\_loss}} + \theta_{12} P_{\mathrm{Diode\_loss}} \quad (1)$$

$$\Delta T_{\mathrm{Diode}} = \theta_{21} P_{\mathrm{IGBT\_loss}} + \theta_{22} P_{\mathrm{Diode\_loss}} \quad (2)$$

where $P_{\mathrm{IGBT\_loss}}$ and $P_{\mathrm{Diode\_loss}}$ are power dissipations in IGBT and diode, respectively. Coefficients θ_{11} and θ_{22} are thermal resistance of IGBT and diode, respectively, while θ_{12} and θ_{21} are thermal coupling coefficients between IGBT and diode.

The junction temperatures of IGBT or diode can be calculated by using the following formula:

$$T_j = T_c + \Delta T = T_a + \theta_a (P_{\mathrm{IGBT\_loss}} + P_{\mathrm{diode\_loss}} + P_{\mathrm{add}}) + \Delta T \quad (3)$$

where T_a and T_c are the ambient temperature and the case temperature, respectively, θ_a is the thermal resistance from ambient to case including the sink, and $P_{\rm add}$ is the power dissipated by other mounted devices in addition to IGBT and diode.

2) Failure Rates of IGBT: An empirical formula recommended by FIDES Guide 2009 can be used to estimate the failure rate of IGBT [19], as follows:

$$\begin{aligned}\lambda_{\rm IGBT} = &(\lambda_{0\rm TH}\Pi_{\rm Thermal} + \lambda_{0\rm TCyCase}\Pi_{\rm TCyCase} \\ &+ \lambda_{0\rm TCySJ}\Pi_{\rm TCySJ} + \lambda_{0\rm RH}\Pi_{\rm RH} \\ &+ \lambda_{0\rm Mech}\Pi_{\rm Mech})\Pi_{\rm Induced}\Pi_{\rm PM}\Pi_{\rm Process} \end{aligned} \tag{4}$$

where $\lambda_{0\rm TH}$ is the basic failure rate of IGBT due to thermal overstress, $\lambda_{0\rm TCyCase}$ to thermal cycling effect on case, $\lambda_{0\rm TCySJ}$ to thermal cycling effect on solder joint, $\lambda_{0\rm RH}$ to humidity, and $\lambda_{0\rm RH}$ to mechanical overstress. Correspondingly, $\Pi_{\rm Thermal}$, $\Pi_{\rm TCyCase}$, $\Pi_{\rm TCySJ}$, $\Pi_{\rm RH}$, and $\Pi_{\rm Mech}$ are the acceleration factors relating to physical overstresses of electrical, thermal, and mechanical origin. $\Pi_{\rm Induced}$ represents the contribution of overstresses cause by other factors, $\Pi_{\rm PM}$ represents the quality of manufactured parts, and $\Pi_{\rm Process}$ represents the quality and technical control over reliability in the product life cycle.

Given the junction temperature information, the temperature factor is calculated by

$$\Pi_{\rm Thermal} = \Pi_{\rm EI} \cdot e^{11604\times 0.7\times[1/293-1/(T_j+273)]} \tag{5}$$

where T_j is junction temperature of IGBT, and

$$\Pi_{\rm EI} = \begin{cases} (V_{\rm applied}/V_{r,\rm IGBT})^{2.4}, & \text{if } (V_{\rm applied}/V_{r,\rm IGBT}) > 0.3 \\ 0.056, & \text{if } (V_{\rm applied}/V_{r,\rm IGBT}) \le 0.3. \end{cases} \tag{6}$$

Here $V_{\rm applied}$ is the applied voltage across IGBT, and $V_{r,\rm IGBT}$ is the rated reverse voltage of IGBT. Typical values of other factors can be found in [19].

It can be seen that the failure rates of IGBTs are related to power loss and system power input levels since the factors are the functions of voltage or temperature while the temperature depends on the power loss that in turn relies on system power input levels.

3) Failure Rates of Diode: A standard reliability model for diode [20] is adopted to estimate the failure rate of diode in PV inverters, as follows:

$$\lambda_D = \lambda_b \pi_T \pi_S \pi_C \pi_Q \pi_E \tag{7}$$

where λ_b is the base failure rate of diode, π_T is the temperature factor, π_S is the electrical stress factor, π_C is the construction factor, and π_Q and π_E are the quality and environment factor, respectively.

Given the junction temperature T_j, the temperature factor is calculated by

$$\pi_T = e^{-3091(1/(T_j+273)-1/298)}. \tag{8}$$

The electrical stress factor [21] can be calculated by

$$\pi_S = \begin{cases} (V_{\rm applied}/V_{r,\rm diode})^{2.45}, & \text{if } 0.3 < V_{\rm applied}/V_{r,\rm diode} < 1 \\ 0.054, & \text{if } V_{\rm applied}/V_{r,\rm diode} \le 0.3 \end{cases} \tag{9}$$

where $V_{\rm applied}$ is the applied voltage across diode, and $V_{r,\rm diode}$ is the rated reverse voltage of diode.

Default values for other factors in (7) can be found in [20]. Similarly, the failure rates of diode are related to power loss and system power input levels through temperature and voltage.

4) Failure Rates of Capacitor: Capacitor failure is a major factor leading to the inverter failure. In particular, PV systems mounted outdoors may suffer from a relatively high failure rate of capacitors because of their exposure to harsher ambient environments. A commonly accepted formula [22] is adopted to compute the failure rate of capacitor, as expressed by

$$\lambda_C = \frac{1}{r_C} = \frac{1}{L_b \cdot 2^{(T_{\max}-T_c)/10}} \tag{10}$$

where r_C is the life expectancy of capacitor, L_b is the base life at elevated maximum core temperature $T_{\max}$ such as 95 °C, and T_c is the actual core temperature. Equation (10) is in agreement with the "life doubles every 10 °C" rule for capacitors, which can be derived from Arrhenius's law [23].

Equation (10) shows that life time estimation for capacitor is a function of core temperature, which mainly depends on the ripple current flowing through the capacitor. Given an inverter without storage component, as shown in Fig. 2, the current ripple can be approximately calculated [24] as follows:

$$i_r(t) = \frac{V_o}{V_d} I_o \cos(2\omega t - \varphi) \tag{11}$$

where V_o and I_o represent the RMS values of grid voltage and output current, V_d is the dc input voltage, ω is the fundamental frequency, and φ is the power factor. Note that higher order harmonics produced by ON/OFF switching are neglected here due to much smaller amplitudes [24].

From (11), the RMS ripple current is

$$I_r = \frac{P_o}{\sqrt{2} V_d} \tag{12}$$

where P_o is the output power of inverter.

The core temperature of capacitor in steady-state [25], therefore, can be calculated by

$$T_c = T_a + \theta_c \left(I_r^2 R_s\right) \tag{13}$$

where R_s is the equivalent series resistance of capacitor, θ_c is the thermal resistance from capacitor core to environment, and T_a is the ambient temperature.

Substituting (13) into (10) yields the power loss related failure rate of capacitor.

5) Inverter Reliability: In general, a PV inverter has no parallel redundancy, meaning a failure in any one component will lead to an outage of the entire inverter. Therefore, the reliability of PV inverter can be modeled as a series network. The failure rate, repair time, and availability of the PV inverter are expressed by

$$\lambda_I(P,V,T) = \lambda_C + \sum_i (\lambda_{Di} + \lambda_{Si}) \tag{14}$$

$$r_I(P,V,T) = \frac{1}{\lambda_I}\left[\lambda_C r_C + \sum_i (\lambda_{Di} r_{Di} + \lambda_{Si} r_{Si})\right] \tag{15}$$

$$A_I(P,V,T) = \frac{1/r_I}{\lambda_I + 1/r_I} \tag{16}$$

where λ_I is the failure rate, r_I is the repair time, A_I is the availability, the subscripts S, D, and C represent IGBT, diode, and capacitor, respectively, and i denotes the ith component. As noted in (14)–(16), all three indices are functions of power flow through the PV inverter, input voltage, and temperature.

In addition, the availabilities of dc disconnect and ac subpanel can be computed from their failure rates and repair times, as follows:

$$A_{\mathrm{DC}} = \frac{1/r_{\mathrm{DC}}}{\lambda_{\mathrm{DC}} + 1/r_{\mathrm{DC}}} \tag{17}$$

$$A_{\mathrm{AC}} = \frac{1/r_{\mathrm{AC}}}{\lambda_{\mathrm{AC}} + 1/r_{\mathrm{AC}}}. \tag{18}$$

The three-phase ac disconnect can be assumed to be perfectly reliable since it is normally closed with very low failure possibility. It can be easily modeled if its failure data is available.

B. Reliability Evaluation of PV Array

1) Equivalent Reliability Parameters of PV String: A PV string is a serial connection of m PV panels and a fuse inside a dc combiner. There are two repairable failure modes for PV panels that result in loss of the whole string: failure at a junction box and short-circuit of PV panel. Both result in outage of a whole PV string until the failure is cleaned. These two failure modes are characterized by an average failure rate and an average repair rate of PV panel. A PV panel may also be bypassed by diodes due to an open failure or shading effect. The bypass of PV panel generally could lower the output of a string, rather than causing an outage of the string. In this paper, we do not consider the bypass of panels in the series formula because this effect is not an outage and has been represented in the input power levels. Moreover, the probability of simultaneous bypass of multiple modules is extremely low, which is negligible. The equivalent reliability parameters of a PV string can be calculated by

$$\lambda_{S,r} = \sum_{i=1}^{m} \lambda_{P,i} + \lambda_F \tag{19}$$

$$r_{S,r} = \frac{1}{\lambda_{S,r}} \left(\sum_{i=1}^{m} \lambda_{P,i} r_{P,i} + \lambda_F r_F \right) \tag{20}$$

$$U_{S,r} = \frac{\lambda_{S,r}}{\lambda_{S,r} + 1/r_{S,r}} \tag{21}$$

where λ and r represent the failure rate and repair time, respectively, and m is the number of PV panels in a PV string. Here the subscripts S, P, F indicate the equivalent PV string, PV panel, and the fuse in the dc combiner, respectively. The subscript r denotes that the calculated reliability parameters are for the reparable failures. $\lambda_{P,i}$ is the failure rate of the ith PV panel, and $r_{P,i}$ is the repair time for the ith PV panel.

2) State Enumeration for Reliability Analysis of PV Array: Once the reliability parameters for all n PV strings in a PV array are obtained, a state enumeration method can be developed to compute reliability parameters of the array. State enumeration is a generic method which is applicable to both homogenous and heterogeneous PV strings.

It is assumed that each PV string has two mutually exclusive states: the working state and out-of-service state. The probabilities of all possible states of a PV array with n strings can be obtained from the expansion of the following expression:

$$(A_{S1} + U_{S1})(A_{S2} + U_{S2}) \cdots (A_{S,n} + U_{S,n}) \tag{22}$$

where n is the number of PV strings in a PV array, and $A_{S,i}$ and $U_{S,i}$ are the availability and unavailability of the ith PV string, respectively. For example, after expansion, the term $(U_{S1} A_{S2} \cdots A_{S,n})$ is the probability of the state of string 1 down but all other strings up; $(A_{S1} \cdots U_{Si} \cdots A_{S,n})$ is the probability of the state of string i down but all other strings up; and so on.

The probability of an enumerated state α of the PV array is calculated by

$$p_A(\alpha) = \prod_{i=1}^{n_f} U_{Si} \prod_{i=1}^{n-n_f} A_{Si} \tag{23}$$

where n_f and $n - n_f$ are the numbers of failed and nonfailed PV strings in state α.

All enumerated states in which j PV strings fail are aggregated into the jth state of the PV array. The probability of the jth state is then expressed by

$$\begin{aligned} p_{Aj} &= \sum_{\alpha \in G(n_f = j)} p_A(\alpha) \\ &= \sum_{\alpha \in G(n_f = j)} \left(\prod_{i=1}^{n_f} U_{Si} \prod_{i=1}^{n-n_f} A_{Si} \right) j = 0, \cdots, n. \end{aligned} \tag{24}$$

In (24), $G(n_f = j)$ denotes the set of enumerated states corresponding to a total of j strings out of service. In particular, State 0 represents the full-up state where all n strings in an array operate properly. State 1 corresponds to the derated state with one PV string out of service ($n - 1$ contingency), State j to the $n - j$ contingency where j-out-of-n PV strings are down ($n - j$ contingency), and State n to the case where all strings in a PV array are out of service. In addition, a full-down state is often due to common causes such as lightning, hail, fire, and other electrical or mechanical problems, but not by independent simultaneous failures of n strings. The common cause failure can be also incorporated into the enumeration process as an additional failure event.

It should be noted that the main purpose of this section is to provide one viable approach to incorporate impacts of system power inputs, voltage levels, and power losses on failure rates of components and in turn on the reliability of whole PV arrays.

III. Discrete Probability Distribution of Input Power

The input power of inverter directly affects the energy losses in IGBT and capacitors, causes variations in temperature inside power electronic devices, and hence impacts the reliability of inverter and energy availability of the PV system. In real-life, the input power of a PV system is normally metered and recorded every 1–15 minutes, which produces a chronological, highly intermittent curve containing a large amount of data points, as illustrated in Fig. 3(a). The input power measurements can be aggregated into a discrete probability distribution [26] to quan-

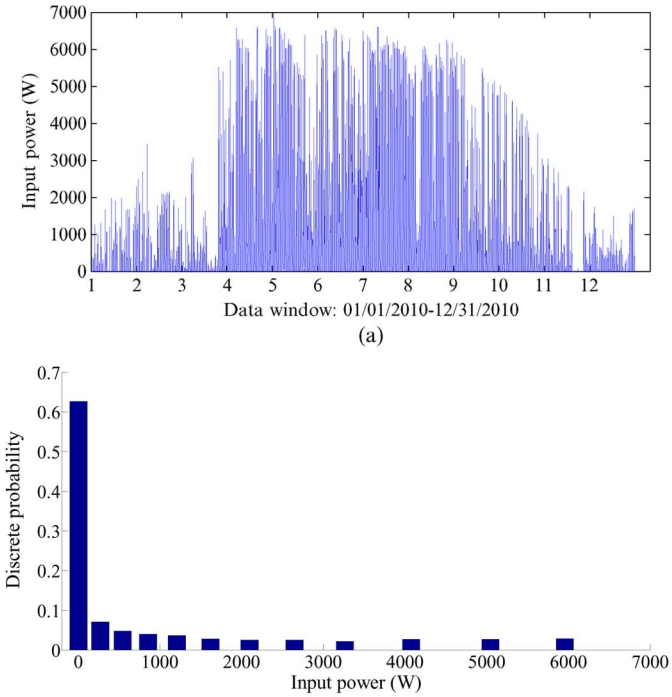

Fig. 3. Power input of phase A. (a) A chronological annual curve; (b) discrete probability distribution of power input.

tify their contribution to long-term reliability of PV systems. To tackle this challenge, a K-mean clustering technique [16] is introduced to eliminate the chronology and to build data points into several power-level groups.

First, assume the annual power curve is to be divided into K power levels. The value of K is adjustable, depending on the level of detail required for reliability analysis. For real-life PV systems, our experiments show that K can be set between 10 and 15, which guarantees satisfactory results depending on cases.

Then, an annual power curve with N data points can be clustered into K power levels in the following steps.

1) Prepare initial clusters $\boldsymbol{S} = \{\boldsymbol{S}_1, \boldsymbol{S}_2, \ldots, \boldsymbol{S}_K\}$ by arbitrarily assigning data points to each cluster; calculate initial cluster mean μ_i, where i corresponds to cluster $\boldsymbol{S}_i$, $i = 1, 2, \ldots, K$.
2) Calculate the distance d_{ji} from each data point P_j $(j = 1, 2, \ldots, N)$ to the ith cluster mean μ_i, i.e.,

$$d_{ji} = |P_j - \mu_i|. \tag{25}$$

3) Assign each data point P_j to the nearest cluster with minimum distance for $j = 1, 2, \ldots, N$; recalculate cluster means by

$$\mu_i = \frac{1}{N_{\boldsymbol{S}_i}} \sum_{P_j \in \boldsymbol{S}_i} P_j, \quad i = 1, 2, \cdots, K \tag{26}$$

where $N_{\boldsymbol{S}_i}$ is the number of data points in the ith cluster.
4) Repeat steps 2 and 3 until each and every μ_i remains unchanged between two iterations.
5) The converged μ_i is the ith mean power level with the discrete probability p_i equaling to N_{S_i}/N, where N is the number of power curves considered. If the time window is a year and sampling interval is 10 min, $N = 8760 \times 6 = 52560$.

For instance, by using the K-mean clustering method, the chronological power curve in Fig. 3(a) is grouped into 12 power levels, and its discrete probability distribution is shown in Fig. 3(b). Each power level in the discrete probability distribution is used to evaluate the reliability parameters of inverter components at that power level and the expected annual energy output and other reliability indices, as detailed in Section IV, are weighted by the probability of each power level.

IV. PV Reliability Indices

The purposes of PV reliability analysis is to evaluate PV system performance and to generate reliability indices that is helpful in selecting the best design option at the planning stage, and is useful in determining measures to reduce cost and increase benefit at the operational stage. To fulfill the goals, two types of reliability indices are introduced: energy-oriented and time-oriented indices.

A. Energy-Oriented Indices

The energy-oriented indices are used to estimate annual PV project yields under uncertain system conditions.

1) Ideal Output Energy (IOE): Ideal output power is the power generated from a 100% reliable PV system, which can be estimated from the clustered power level by applying the converter efficiency curve. Therefore, the IOE is obtained by

$$\text{IOE} = \sum_{l} \sum_{i=1}^{K} \mu_i \eta_i p_i D \tag{27}$$

where K is the number of input power levels for a single phase, and the subscript i denotes the ith input power level. Therefore, μ_i is the mean of the ith input power level, η_i is the efficiency of PV inverter at μ_i, p_i is the probability of the ith power level, and D is the total time duration considered. If the annual IOE is considered, then $D = 8760$ h. The subscript l represents the lth phase in a three-phase PV system. The total output power of the three-phase PV system equals the sum of the power of each individual phase. Note that the subscript l denoting the lth phase for each variable in (27) is omitted for simplicity. Unless specifically noted, the subscript l for the lth phase is always omitted in this paper.

2) Expected Output Energy (EOE): With nonperfect reliability, the expected power output of the PV system is the ideal output multiplying the system availability. Numerically, the sum of the expected output at each power level multiplied by the probability of each power level gives the total expected output energy. Applying this general idea to the central inverter system gives

$$\text{EOE} = \sum_{l} \left[\sum_{i=1}^{K} \eta_i p_i D \sum_{j \in \{0,1,2,\cdots,n-1\}} \times f_j \mu_i p_{Aj} A_{I,ij}(f_j \mu_i, V_{\text{DC},i}) \right] A_{\text{DC}} A_{\text{AC}} \tag{28}$$

where p_{Aj} is the probability of the jth state of the PV array, A_{Iij} is the availability of the inverter at the ith input power level and the jth state of the PV array, $f_j\mu_i$ represents the expected input power of inverter after considering PV array failures, and $A_{\rm DC}$ and $A_{\rm AC}$ denote the availability of the dc disconnect and ac subpanel, respectively. Here f_j is a ratio that takes the value 1 for State 0, $(n-1)/n$ for State 1, $(n-2)/n$ for State 2, and $(n-j)/n$ for State j, if the PV array is composed of n homogeneous strings. Obviously, A_{Iij} is a function of input power $f_j\mu_i$ and inverter dc side voltage $V_{{\rm DC},i}$.

3) Energy Availability (A_e): The A_e is defined as normalized EOE on the basis of IOE

$$A_e = \frac{\rm EOE}{\rm IOE}. \tag{29}$$

It is worth noting that the physical meaning of A_e is totally different from that of A_t proposed in the next subsection. A_e is proposed from the angle of energy generation. When some of the PV strings fail but others still function, the PV system still partially generates energy and hence this scenario is still counted in A_e. However, A_t is constructed on the basis of repair time requirement. Only the states of whole system functioning contribute to A_t. In other words, the probabilities of the states in which some of the PV strings fail but others still generate energy are excluded from A_t. In this sense, A_e is more benefit- or yield-oriented, whereas A_t is more cost-oriented reflecting the time and effort to restore the PV system back to the normal state.

B. Time-Oriented Indices

The time-oriented indices are introduced to quantify the annual outage time and annual available time, which are useful for justifying maintenance requirements for PV systems.

1) Time Availability (A_t): A_t is a relative measure of how many hours the PV power system is expected to operate in normal conditions every year and can be calculated by

$$A_t = \prod_l \left[\sum_{i=1}^{K} p_i p_{A0} A_{I,i0}(f_0\mu_i, V_{{\rm DC},i}) A_{\rm DC} A_{\rm AC}\right]. \tag{30}$$

A_t gives the percentage time when the whole PV system stays intact without needing repair or replacement. Note that the time availability includes the time when the PV system has a zero MW output due to no solar insolation.

The time availability for a single phase can be calculated by the items enclosed within the bracket in (30). Note that the subscript l for the lth phase in each variable is omitted in (30).

The unavailability is calculated by

$$U_t = 1 - A_t. \tag{31}$$

The unavailability in (31) includes the probabilities that the PV power system operates in various derated states with part of the PV strings out of service (e.g., $n-1$, $n-2$ conditions, etc.). The probability for the single derated state can also be obtained by the state enumeration method if necessary.

2) Available ($H_{\rm av}$), Derated ($H_{\rm dr}$), and Outage Hours ($H_{\rm dw}$): The fully available hours $H_{\rm av}$ are calculated by

$$H_{\rm av} = A_t \cdot 8760. \tag{32}$$

$H_{\rm dw}$ gives the average time in hours for whole plant shutdown and is calculated as follows:

$$H_{\rm dw} = 8760 \prod_l \left[1 - \sum_{i=1}^{K} p_i \sum_{j\in\{0,1,2,\cdots,n-1\}} \times p_{Aj} A_{I,ij}(f_j\mu_i, V_{{\rm DC},i}) A_{\rm DC} A_{\rm AC}\right]. \tag{33}$$

The total time in hours of the PV system in derated states is calculated by

$$H_{\rm dr} = 1 - H_{\rm av} - H_{\rm dw}. \tag{34}$$

The time-oriented reliability indices help one understand the health condition of the PV system and perform intelligent asset management.

C. Simple Example

A simplified single-phase PV system is used as an example to clarify the physical meaning of (27)–(34). It is assumed that the PV system consists of one inverter and two strings with two modules in each string. The input power is clustered to two levels only.

From (27), the ideal output energy (IOE) is expressed by

$$\rm IOE = \mu_1\eta_1 p_1 D + \mu_2\eta_2 p_2 D \tag{35}$$

where μ_1 and μ_2 are the average of the two input power levels clustered, and η_1 and η_2 represent the efficiency of inverter at two different power levels, respectively. Hence $\mu_1\eta_1$ and $\mu_2\eta_2$ denote the mean of output power. Accordingly, $p_1 D$ and $p_2 D$ are the expected duration of the two power levels within a specified total period of study.

According to (22), two strings have four enumerated states respectively with their probabilities of $A_{S1}A_{S2}$, $A_{S1}U_{S2}$, $U_{S1}A_{S2}$, and $U_{S1}U_{S2}$. The four states can be further simplified to the nonfailure state, combined one-string failure state and two-string failure state. The probability of the combined one-string failure equals the sum of $A_{S1}U_{S2}$ and $U_{S1}A_{S2}$. By using the subscripts 0, 1, and 2 to represent the nonstring failure state, combined one-string failure state, and two-string failure state, respectively, and by assuming two PV strings have the same availability and unavailability, the expected output energy calculated by (28) is

$$\begin{aligned}\rm EOE &= \sum_{i=1}^{2} \eta_i p_i D \sum_{j\in\{0,1,2\}} f_j\mu_i p_{Aj} A_{I,ij}(f_j\mu_i, V_{{\rm DC},i}) A_{\rm DC} A_{\rm AC} \\ &= p_1 D\left[\eta_1(f_0\mu_1 p_{A0} A_{I,10} + f_1\mu_1 p_{A1} A_{I,11}) A_{\rm DC} A_{\rm AC}\right] \\ &\quad + p_2 D\left[\eta_2(f_0\mu_2 p_{A0} A_{I,20} + f_1\mu_2 p_{A1} A_{I,21}) A_{\rm DC} A_{\rm AC}\right]\end{aligned} \tag{36}$$

where f_0 and f_1 are the coefficients for the input power of inverter corresponding to the nonstring failure state and combined one-string failure state, respectively. Note that the two-string failure state does not contribute to EOE because no power is generated under this situation. Accordingly, p_{A0} and p_{A1} are the probabilities of the nonstring failure and combined one-string

TABLE I
RELIABILITY INDICES FOR BASE CASES

Energy Indices	*EOE* (MWh)	*IOE* (MWh)	A_e
	20.06	20.265	0.990237
Time Indices	A_t	H_{av} (hrs)	H_{dr} (hrs)	H_{dw} (hrs)
	0.90682	7943.74	816.26	4e-6

failure states, and $A_{I,10}, A_{I,11}$ and $A_{I,20}, A_{I,21}$ are the availabilities of inverter corresponding to these two failure states when considering the PV array's output at power levels 1 and 2. It is worth remembering that $A_{I,ij}$ is the function of the input power $(f_j\mu_i)$ and operational voltage $(V_{\mathrm{DC},i})$. However, for the purpose of simplification, $f_j\mu_i$ and $V_{\mathrm{DC},i}$ are not explicitly expressed in the expanded form of (36). The expression in the brackets denotes the expected output power at a specific power level, where all possible component failures in the PV system are taken into account. The total expected output energy is the sum of the product of the expected output power and duration at each power level.

According to the definition of A_t, (30) can be expanded as

$$A_t = p_1 p_{A0} A_{I,10} A_{\mathrm{DC}} A_{\mathrm{AC}} + p_2 p_{A0} A_{I,20} A_{\mathrm{DC}} A_{\mathrm{AC}} \quad (37)$$

where only the normal state without any failure in the PV system contributes to the time availability index.

Similarly, (33) is expanded into (38), shown at the bottom of the page.

V. TEST RESULTS

Reliability analyses are performed using a real-life central-inverter PV system connected to the BC Hydro distribution network. Fig. 1 shows the schematic diagram of a 20-kW three-phase PV power system connected to the BC Hydro distribution grid, which is located in Langley, BC, Canada. The PV system consists of a total of 18 strings in three phases, with 96 PV modules in series in each string. The central inverter in each phase has a maximum capacity of 7 kW and a nominal ac voltage of 208 V. Fig. 3(a) illustrates the annual power outputs of the central inverter, whereas Fig. 3(b) is the 12 power level model of the output obtained using the clustering technique. Note that, in the test cases, it is not necessary to apply inverter efficiency curve on the power input because the inverter output has been directly measured. Reliability parameters of the PV system are summarized in Table A-I in the Appendix, whereas the discrete probability model for annual power outputs of the PV system is given in Table A-II.

A. Reliability Results for Base Case

By using the reliability parameters in Table A-I, the reliability results for the base case are obtained, as listed in Table I.

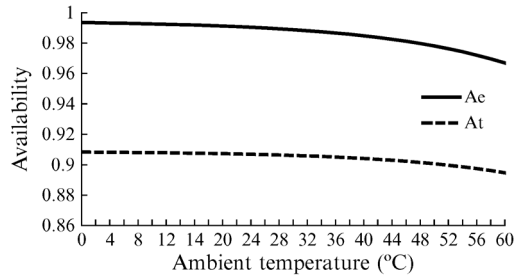

Fig. 4. Temperature effect on energy availability and time availability.

The results show that the energy availability of the test system is as high as 99.02% in contrast to a time availability of only 90.68%. The rationale behind the results is that any derated states or partial failures of the PV system are counted in the time unavailability. On the other hand, the PV system is still able to generate electricity during derated hours, resulting in relatively higher energy availability.

B. Temperature Impact on PV Reliability

The temperature impact on PV system reliability was explored. The central inverter in the test PV system is located inside an electrical room with cooling facilities. In the sensitivity study, the effective ambient temperature for the central inverter is assumed to vary between 0 °C and 40 °C. Reliability results with temperatures from 40 °C and 60 °C are also calculated to obtain some benchmark results for outdoor central inverter systems for which the ambient temperature may rise up to 60 °C considering their direct exposure to sunlight and working in high heat emitted by PV panels.

The sensitivity results are illustrated in Fig. 4. The reliability results for lower temperature are not listed because the changes in reliability results are not appreciable when the temperature is below 0 °C. It can be observed from Fig. 4 that:

1) The reliability level of the PV system is reduced with temperature rise. The A_e decreases from 99.36% to 96.69% due to temperature changes from 0 °C to 60 °C.
2) The time availability index A_t also drops with temperature rise. This means that outage time increases under a higher temperature condition, implying that more maintenance activities are required. A_e is more sensitive to temperature than A_t.

C. Insolation Effect on PV Reliability

Solar insolation directly determines the power input of PV inverter, which in turn affects power loss in IGBTs, diodes, and the capacitor. Qualitatively, insolation rise will cause an increase of junction temperatures in IGBT and diode and core temperature

$$H_{\mathrm{dw}} = 8760 \prod_{l} \left[1 - \sum_{i=1}^{2} p_i \sum_{j\in\{0,1\}} p_{Aj} A_{I,ij}\,(f_j\mu_i, V_{\mathrm{DC},i}) A_{\mathrm{DC}} A_{\mathrm{AC}} \right]$$
$$= 8760 \cdot [1 - (p_1 p_{A0} A_{I,10} A_{\mathrm{DC}} A_{\mathrm{AC}} + p_1 p_{A1} A_{I,11} A_{\mathrm{DC}} A_{\mathrm{AC}} + p_2 p_{A0} A_{I,20} A_{\mathrm{DC}} A_{\mathrm{AC}} + p_2 p_{A1} A_{I,21} A_{\mathrm{DC}} A_{\mathrm{AC}})] \quad (38)$$

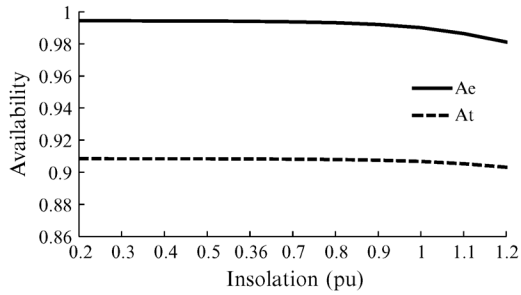

Fig. 5. Insolation effect on energy availability and time availability.

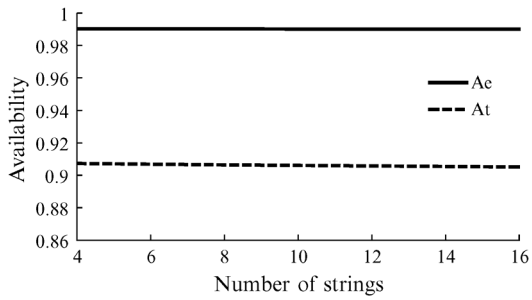

Fig. 6. Availability as a function of number of strings.

of the capacitor, and therefore, will eventually lead to a higher failure rate of the inverter. The effect of insolation on PV system reliability is quantified by changing the input power of inverter from 0.2 to 1.2 times of the base case input. Fig. 5 illustrates the sensitivity study results for insolation effects.

It can be seen from Fig. 5 that:

1) The test PV system is vulnerable to the variations in insolation intensity. The energy availability A_e decreases from 99.024% to 98.119% due to insolation increase from 1.0 per unit (the nominal value) to 1.2 per unit.
2) Insolation rise causes a relatively large variation after the rating capacity (1.0 p.u.) in outage time of the PV system. The reason is that a higher insolation level will create a nonlinear rise of inverter failure rate.

D. Reliability as a Function of Number of PV Strings

A frequently asked question is whether the PV system reliability can be enhanced by a more distributed design? This is investigated by varying the number of strings n in the PV array while keeping the output capacity of each phase array at 7 kW and the total output of the three-phase PV system at 20 kW after considering the highest efficiency of inverter 97.1%. The reliability analysis results are shown in Fig. 6.

It can be seen from Fig. 6 that both A_e and A_t for the PV system are insensitive to the increased n. On the one hand, the failure rate of each string will reduce with the number of panels. On the other hand, more contingencies of strings will occur as n increases. These two opposite effects are almost offset in this case. This is a desirable feature showing that the centralized PV design has a robust reliability performance and hence a relatively stable maintenance cost unaffected by PV array configurations.

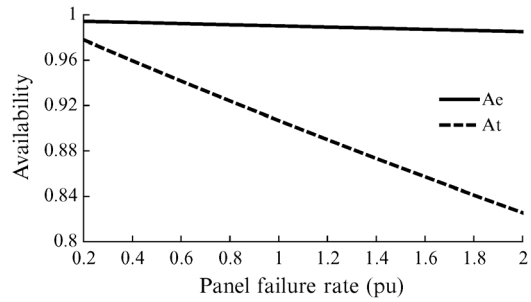

Fig. 7. Sensitivity of system reliability with respect to panel failure rate.

E. Effect of Panel Failure Rate on PV Reliability

The sensitivity analysis results of changing the failure rate of PV panel λ_p are shown in Fig. 7. It can be observed that the reliability of the test PV system is sensitive to λ_p, particularly for A_t because each PV string consists of many PV panels in series. In the studied case, there are 96 panels in one string.

In addition, it may be worth pointing out that the sensitivity curve for the repair time of the PV panel is the same as those for the failure rate of the PV panel. This is because the availability of the PV panel is equal to $1/(1+\lambda_p r_p)$, where the two variables are exchangeable.

Reliability sensitivity with respect to inverter repair time is also analyzed. Moreover, the reliability performances of the central inverter PV system and string inverter PV system are compared. Those results are omitted due to limited space.

F. Effect of PV Degradation and Aging Failure

In general, the life of PV modules can be as high as 25 years for most commercial products. PV degradation over time and aging failures should be considered in reliability analysis whenever a PV module approaches the final stage of useful life.

In this paper, it is assumed that the efficiency of the PV module degrades linearly with a constant slope [27], i.e., the power output of the PV array decreases over years as follows:

$$p_i = p_0\,[1-(k-1)d] \quad k = 1, \ldots, L \tag{39}$$

where p_0 is the initial power capacity of a PV module, d is the constant slope, k represents a specified service year, and L is the observed life cycle.

The aging failure model proposed in [28] is adopted to calculate the yearly increased unavailability due to aging failure (see Appendix B). It is assumed that the life of the PV array obeys a normal probability distribution with 25 years of mean (μ_A) and 5 years of variance (σ_A). For a PV string considering both reparable and nonreparable failures, the total unavailability can be obtained by using the union concept. It is noted that IOE is always set to be a constant of the energy generated in the first service year in computing the annual energy availability index A_e using (29).

The changes of the system indices A_e and A_t over years considering both degradation and aging failures are shown in Fig. 8. It can be seen that A_e and A_t are much more sensitive to the service age than other reliability parameters. At the end of predicted useful life of PV array, the values of A_e and A_t are

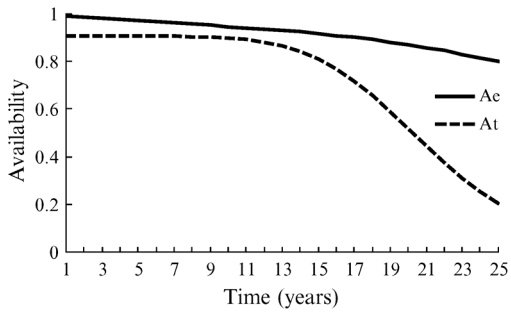

Fig. 8. System reliability for 25 years considering degradation and aging failures.

very low, especially for A_t, which represents a higher repair and maintenance demand.

A_t is insensitive to the increase of service age in the first 15 years, but quickly goes down while approaching toward the average life of a PV array. In contrast to A_t, the decreasing trend of A_e is smoother. The phenomenon reveals that A_e can directly catch the change of PV degradation and aging failure. However, A_t mainly reflects the influence of aging failure rather than PV degradation because PV degradation can only indirectly impact A_t through changes in the input power of inverter.

VI. Conclusions

A new analytical technique is proposed to evaluate the reliability performance of grid-connected PV power systems. The major contributions include the development of power input/power loss/temperature-dependent failure rates for power electronic components in the PV system, the reliability evaluation method for PV arrays considering power output-dependent failure rates of system components, and application of a clustering technique to the discrete probability distribution model of solar power outputs. Reliability performance indices are defined to quantify the energy output availability and average outage time of the PV system.

The effectiveness of the proposed method has been validated using a real-life 20-kW grid-connected PV system. Sensitivities of PV system reliability to system structure, temperature variation, solar insolation, number of PV strings, and PV panel failure rate are analyzed. Application of the proposed method to actual PV systems can provide valuable information that is useful to enhance PV system reliability, to choose better PV system design options, and to realize maximum benefit of PV power.

Appendix

A. Loss Estimation for IGBT and Diode

Power losses in IGBT and diode are the sum of the following conduction losses and switching losses.

1) Conduction Losses:

$$P_{\mathrm{IGBT-cond}} = \frac{1}{2} I_M V_{1o}\left(\frac{1}{\pi} + \frac{\mu}{4}\cos\varphi\right) + \frac{a_1}{4\sqrt{\pi}} I_M^{(b_1+1)}\left[\frac{\Gamma\left(\frac{b_1+2}{2}\right)}{\Gamma\left(\frac{b_1+3}{2}\right)} + \frac{\Gamma\left(\frac{b_1+3}{2}\right)}{\Gamma\left(\frac{b_1+2}{2}+1\right)}\mu\cos\varphi\right] \quad \text{(A-1)}$$

$$P_{\mathrm{DIODE-cond}} = \frac{1}{2} I_M V_{2o}\left(\frac{1}{\pi} - \frac{\mu}{4}\cos\varphi\right) + \frac{a_2}{4\sqrt{\pi}} I_M^{(b_2+1)}\left[\frac{\Gamma\left(\frac{b_2+2}{2}\right)}{\Gamma\left(\frac{b_2+3}{2}\right)} - \frac{\Gamma\left(\frac{b_2+3}{2}\right)}{\Gamma\left(\frac{b_2+2}{2}+1\right)}\mu\cos\varphi\right] \quad \text{(A-2)}$$

where Γ is the Gamma function, V_{1o}, a_1, b_1, V_{2o}, a_2, and b_2 are model parameters to calculate voltage drop across IGBT and diode (see [17]), I_M and φ are current magnitude and power factor at the inverter output interface, and μ represents modulation index.

2) Switching Losses:

(i) Losses in the active device with an ideal diode without considering reverse recovery

$$P_{\mathrm{on}} = f h I_M^k \frac{1}{2\sqrt{\pi}} \frac{\Gamma\left(\frac{k+1}{2}\right)}{\Gamma\left(\frac{k}{2}+1\right)} k_{g\mathrm{on}} \frac{V_{\mathrm{applied}}}{V_t} \quad \text{(A-3)}$$

$$P_{\mathrm{off}} = f z I_M^r \frac{1}{2\sqrt{\pi}} \frac{\Gamma\left(\frac{r+1}{2}\right)}{\Gamma\left(\frac{r}{2}+1\right)} k_{g\mathrm{off}} \frac{V_{\mathrm{applied}}}{V_t} \quad \text{(A-4)}$$

where f is the operating frequency for IGBT; the symbols h, k and z, r are the model parameters for the calculation of switching energy loss. $k_{g\mathrm{on}}$ and $k_{g\mathrm{off}}$ correspond to gate drive impedance in ON and OFF states, respectively, and V_t is the test voltage and V_{applied} is related to the applied voltage.

(ii) Contribution of the diode reversed recovery

$$E_{\mathrm{IGBT-RR}} = V_{\mathrm{applied}} I_L \left[\left(1 + \frac{1}{2}\frac{I_{rr}}{I_L}\right) t_a + \frac{1}{4}\frac{I_{rr}}{I_L} t_b\right] \quad \text{(A-5)}$$

where V and I_L are the applied voltage and average current, and I_{rr} is the peak reverse recovery current. For each switching-cycle, it is assumed that the voltage across the diode stays close to $0V$ during the length of t_a and rises to the applied voltage during t_b.

3) Diode Switching Losses:

$$E_{\mathrm{IGBT-sw}} = 0.5 I_{rr} \cdot 0.5 V \cdot t_b. \quad \text{(A-6)}$$

The instant power losses due to diode reversed recovery and diode switching can be obtained by multiplying the corresponding energy losses by the operating frequency.

B. Aging Failure Model

Given a failure density probability function $f(t)$, the probability of transition to aging failure of a component in a subsequent period t after having survived for T years can be calculated by

$$P_{T,t} = \frac{\int_T^{T+t} f(t)dt}{\int_T^{\infty} f(t)dt}. \quad \text{(A-7)}$$

Further dividing t into N small intervals with the same length Δx, the failure probabilities in all the intervals can be calculated by

$$P_i = \frac{\int_T^{T+i\Delta x} f(t)dt - \int_T^{T+(i-1)\Delta x} f(t)dt}{\int_T^{\infty} f(t)dt} \ (i = 1, 2, \ldots, N). \tag{A-8}$$

If a failure happened in the ith interval, the corresponding average unavailability duration is

$$\mathrm{UD}_i = t - (2i-1)\Delta x/2 \quad (i = 1, 2, \ldots, N). \tag{A-9}$$

The component unavailability in a specified subsequent t period is

$$U_{T,t} = \sum_{i=1}^{N} P_i \cdot \mathrm{UD}_i / t. \tag{A-10}$$

In general, t is selected as one year period and the aging failure can be modeled by *a posteriori* normal distribution or *a posteriori* Weibull distribution [16].

The equivalent reliability parameters of the PV string considering both reparable failure and aging failure can be yielded using the union concept

$$U_S = U_{S,r} + U_{T,t} - U_{S,r}U_{T,t} \tag{A-11}$$

$$A_S = 1 - U_S \tag{A-12}$$

where $U_{S,r}$ and $U_{T,t}$ are the unavailability due to reparable and nonreparable failures, respectively; A_S and U_S are the total availability and unavailability of PV string, respectively.

C. Reliability Parameters for the PV Power System Connected to the BC Hydro Grid

TABLE A-I
PARAMETERS FOR RELIABILITY ANALYSIS OF BASE CASE

IGBT & Diode					
T_a(°C)	μ	$cos\varphi$	V_t(V)	f(kHz)	
25	0.8	0.95	480	20	
P_{add}(W)	θ_a(°C/W)	V_{1o}(V)	a_1	b_1	
11	0.11	0.9654	0.1642	0.6468	
k	z	h	r	$V_{r,\ IGBT}$(V)	
1.6783	0.0181	0.0040	1.3444	480	
θ_{11}(°C/W)	θ_{12}(°C/W)	θ_{21}(°C/W)	θ_{22}(°C/W)	r_{Di}(days)	
0.640	0.250	0.300	0.830	20	
λ_{0TH}	$\Pi_{Induced}$	Π_{PM}	$\Pi_{Process}$	r_{Si}(days)	
0.3021	2.0	1.7	4.0	20	
k_{goff}	k_{gon}	$V_{r,\ diode}$(V)	t_a(ns)	t_b(ns)	
1.0	1.5	600	25.9	54.1	
V_{2o}(V)	a_2	b_2	I_{rr}(A)		
0.711	0.136	0.395	10		
λ_b	π_E	π_C	π_Q		
0.005	6.0	1.0	2.4		
Capacitor					
L_b(hours)	T_{max}(°C)	R_s(Ω)	θ_c(°C/W)	r_C(days)	
20000	95	0.02	15.6	10	
PV array					
$\lambda_{P,i}$	$r_{P,i}$	λ_F	r_F	d	μ_A(years)	σ_A(years
1.1416	48	5.7078	10	0.5%	25	5
DC disconnect and AC subpanel					
λ_{DC}	r_{DC}	λ_{AC}	r_{AC}		
0.05	16	0.01	10		

Note: The unit for the failure rates is $1/(10^6$ h) and repair time is hours.

D. Clustered Inverter Output Power Levels and Probabilities

TABLE A-II
CLUSTERED POWER LEVELS AND ASSOCIATED DC VOLTAGES AND PROBABILITIES DERIVED FROM ANNUAL INVERTER OUTPUT CURVE

Mean \ Level i	1	2	3	4	5	6
$\mu_i\eta_i$(W)	274	860	1212	2652	5049	3269
$V_{d,i}$(V)	384	394	392	371	334	365
p_i	0.071	0.040	0.036	0.025	0.026	0.021
Mean \ Level i	7	8	9	10	11	12
$\mu_i\eta_i$(W)	5960	4078	2102	1622	549	6.62
$V_{d,i}$(V)	319	351	379	388	391	74
p_i	0.028	0.027	0.025	0.028	0.047	0.626

REFERENCES

[1] J. L. Sawin and E. Martinot, Renewables 2010 Global Status Report Renewable Energy Policy Network for the 21st Century, 2010.

[2] A. Ristow, M. Begovic, A. Pregelj, and A. Rohatgi, "Development of a methodology for improving photovoltaic inverter reliability," *IEEE Trans. Ind. Electron.*, vol. 55, no. 7, pp. 2581–2592, Jul. 2008.

[3] E. Roman, R. Alonso, P. Ibanez, S. Elorduizapatarietxe, and D. Goitia, "Intelligent PV module for grid-connected PV systems," *IEEE Trans. Ind. Electron.*, vol. 53, no. 4, pp. 1066–1073, Jun. 2006.

[4] P. Lall, "Tutorial: Temperature as an input to microelectronics—Reliability models," *IEEE Trans. Reliability*, vol. 45, no. 1, pp. 3–9, Mar. 1996.

[5] M. Vazquez and I. Rey-Stolle, "Photovoltaic module reliability model based on field degradation studies," *Prog. Photovoltaics: Res. Applicat.*, vol. 16, no. 5, pp. 419–433, Aug. 2008.

[6] V. Smet, F. Forest, and J. J. Huselstein, "Ageing and failure modes of IGBT modules in high temperature power cycling," *IEEE Trans. Ind. Electron.*, accepted for publication.

[7] J. Liu and N. Henze, "Reliability consideration of low-power grid-tied inverter for photovoltaic application," in *Proc. 24th Eur. Photovoltaic Solar Energy Conference and Exhibition*, Hamburg, Germany, Sep. 2009.

[8] G. Petrone, G. Spagnuolo, R. Teodorescu, M. Veerachary, and M. Vitelli, "Reliability issues in photovoltaic power processing systems," *IEEE Trans. Ind. Electron.*, vol. 55, no. 7, pp. 2569–2580, Jul. 2008.

[9] L. H. Stember, W. R. Huss, and M. S. Bridgman, "A methodology for photovoltaic system reliability & economic analysis," *IEEE Trans. Reliability*, vol. 31, no. 3, pp. 296–303, Aug. 1982.

[10] S. V. Dhople, A. Davoudi, P. L. Chapman, and A. D. Domínguez-García, "Integrating photovoltaic inverter reliability into energy yield estimation with Markov models," in *Proc. 2010 IEEE 12th Workshop on Control and Modeling for Power Electronics (COMPEL)*, Boulder, CO, Jun. 2010, pp. 1–5.

[11] E. Collins, M. Dvorack, J. Mahn, M. Mundt, and M. Quintana, "Reliability and availability analysis of a fielded photovoltaic system," in *Proc. 34th IEEE Photovolt. Spec. Conf.*, 2009, pp. 316–2321.

[12] A. Pregelj, M. Begovic, and A. Rohatgi, "Impact of inverter configuration on PV system reliability and energy production," in *Proc. 29th IEEE Photovolt. Spec. Conf.*, 2002, pp. 1388–1391.

[13] E. L. Meyer and E. E. van Dyk, "Assessing the reliability and degradation of photovoltaic module performance parameters," *IEEE Trans. Reliability*, vol. 53, no. 1, pp. 83–92, Mar. 2004.

[14] D. Hirschmann, D. Tissen, S. Schröder, and R. W. De Doncker, "Reliability prediction for inverters in hybrid electrical vehicles," *IEEE Trans. Power Electron.*, vol. 22, no. 6, pp. 2511–2517, Nov. 2007.

[15] W. Xiao, N. Ozog, and W. G. Dunford, "Topology study of photovoltaic interface for maximum power point tracking," *IEEE Trans. Ind. Electron.*, vol. 54, no. 3, pp. 1696–1704, Jun. 2007.

[16] W. Li, *Risk Assessment of Power Systems: Models, Methods, and Applications*. New York: IEEE Wiley, 2005.

[17] S. Clemente, "A simple tool for the selection of IGBTs for motor drives and UPSs," in *Proc. IEEE Applied Power Electronics Conf. Exposition*, Mar. 1995, pp. 755–764.

[18] Z. Luo, H. Ahn, and M. A. E. Nokali, "A thermal model for insulated gate bipolar transistor module," *IEEE Trans. Power Electron.*, vol. 19, no. 4, pp. 902–907, Jul. 2004.

[19] FIDES Group, FIDES Guide 2009, Issue A, Reliability Methodology for Electronic Systems 2009.
[20] U.S. DOD, Military Handbook MIL-HDBK-217 Notice 2, Reliability Prediction of Electronic Equipment Washington, DC, Feb. 1995.
[21] U.S. DOD, Military Handbook MIL-HDBK-217F, Reliability Prediction of Electronic Equipment Washington, DC, Dec. 1991.
[22] S. G. Parler, Jr., "Deriving life multipliers for electrolytic capacitors," *IEEE Power Electron. Soc. Newslett.*, vol. 16, no. 1, pp. 11–12, Feb. 2004.
[23] A. Albertini, M. G. Masi, G. Mazzanti, L. Peretto, and R. Tinarelli, "Toward a BITE for real-time life estimation of capacitors subjected to thermal stress," *IEEE Trans. Instrum. Meas.*, vol. 60, no. 5, pp. 1674–1681, May 2011.
[24] M. H. Rashid*, Power Electronics Handbook: Devices, Circuits, and Applications*, 2nd ed. New York: Academic, 2007.
[25] *Application Guide, Aluminum Electrolytic Capacitors*. Liberty, SC: Cornell Dubilier, 2003 [Online]. Available: http://www.cornell-dubilier.com/appguide.pdf
[26] A. Haldar and S. Mahadevan*, Probability, Reliability, and Statistical Methods in Engineering Design*. Hoboken, NJ: Wiley, 2000.
[27] M. Vazquez and I. Rey-Stolle, "Photovoltaic reliability model based on field degradation studies," *Prog. Photovolt: Res. Appl.*, vol. 16, no. 5, pp. 419–433, Aug. 2008.
[28] W. Li, "Incorporating aging failure in power system reliability evaluation," *IEEE Trans. Power Syst.*, vol. 17, no. 3, pp. 918–923, Aug. 2002.

Peng Zhang (M'07–SM'10) received the Ph.D. degree from the University of British Columbia, Vancouver, BC, Canada.

He is an Assistant Professor of Electrical Engineering at the University of Connecticut, Storrs. He was a System Planning Engineer at BC Hydro and Power Authority, Vancouver, Canada. His research interests include power system reliability, renewable energy integration, and wide area measurement and control systems.

Dr. Zhang is a Registered Professional Engineer in British Columbia, Canada.

Yang Wang received the Ph.D. degree from Chongqing University, China.

Currently, he is a postdoctoral fellow in the Department of Electrical and Computer Engineering at the University of Connecticut, Storrs. His research interests include wide-area measurement system, voltage stability, and photovoltaic power system.

Weidong Xiao (M'07) received the M.Sc. and Ph.D. degrees from the University of British Columbia, Vancouver, BC, Canada.

He is an Assistant Professor of Electrical Power Engineering at Masdar Institute of Science and Technology. Before his academic career, he worked with MSR Innovations Incorporation as a R&D engineering manager focusing on projects related to integration, monitoring, evaluation, optimization, and design of photovoltaic power systems. His research area includes power electronics, photovoltaic power systems, digital control techniques, and industrial applications.

Wenyuan Li (F'02) is a Principal Engineer at BC Hydro, Vancouver, Canada.

Dr. Li is a Fellow of Canadian Academy of Engineering and Engineering Institute of Canada. He has published five books and over 140 papers in power system planning, probabilistic applications, and reliability. He is an editor of IEEE TRANSACTIONS ON POWER SYSTEMS and IEEE POWER ENGINEERING LETTERS, and has received several IEEE awards including the IEEE PES Roy Billinton Power System Reliability Award in 2011.